AFRL-RZ-WP-TP-2008-2113

EFFECTS OF PULSED-D.C. DISCHARGE PLASMA ACTUATORS IN A SEPARATED LOW PRESSURE TURBINE BOUNDARY LAYER (POSTPRINT)

J.D. Wall, I.C. Boxx, R.B. Rivir, and M.E. Franke

Turbine Branch
Turbine Engine Division

JANUARY 2007

AIR FORCE RESEARCH LABORATORY
PROPULSION DIRECTORATE
WRIGHT-PATTERSON AIR FORCE BASE, OH 45433-7251
AIR FORCE MATERIEL COMMAND
UNITED STATES AIR FORCE

REPORT DOCUMENTATION PAGE

Form Approved
OMB No. 0704-0188

1. REPORT DATE *(DD-MM-YY)*	2. REPORT TYPE	3. DATES COVERED *(From - To)*
January 2007	Conference Paper Postprint	01 January 2003 – 10 January 2007

4. TITLE AND SUBTITLE
EFFECTS OF PULSED-D.C. DISCHARGE PLASMA ACTUATORS IN A SEPARATED LOW PRESSURE TURBINE BOUNDARY LAYER (POSTPRINT)

5a. CONTRACT NUMBER
In-house

5b. GRANT NUMBER

5c. PROGRAM ELEMENT NUMBER
61102F

6. AUTHOR(S)
J.D. Wall and M.E. Franke (Air Force Institute of Technology)
I.C. Boxx and R.B. Rivir (RZTT)

5d. PROJECT NUMBER
2307

5e. TASK NUMBER
06

5f. WORK UNIT NUMBER
2307S314

7. PERFORMING ORGANIZATION NAME(S) AND ADDRESS(ES)
Air Force Institute of Technology
Wright-Patterson Air Force Base, OH 45433

Turbine Branch (AFRL/RZTT)
Turbine Engine Division
Air Force Research Laboratory, Propulsion Directorate
Wright-Patterson Air Force Base, OH 45433-7251
Air Force Materiel Command, United States Air Force

8. PERFORMING ORGANIZATION REPORT NUMBER
AFRL-RZ-WP-TP-2008-2113

9. SPONSORING/MONITORING AGENCY NAME(S) AND ADDRESS(ES)
Air Force Research Laboratory
Propulsion Directorate
Wright-Patterson Air Force Base, OH 45433-7251
Air Force Materiel Command
United States Air Force

10. SPONSORING/MONITORING AGENCY ACRONYM(S)
AFRL/RZTT

11. SPONSORING/MONITORING AGENCY REPORT NUMBER(S)
AFRL-RZ-WP-TP-2008-2113

12. DISTRIBUTION/AVAILABILITY STATEMENT
Approved for public release; distribution unlimited.

13. SUPPLEMENTARY NOTES
Conference paper published in the Proceedings of the 45th AIAA Aerospace Sciences Meeting and Exhibit, January 8 - 11, 2007, in Reno, Nevada. Technical paper contains color. PAO Case Number: AFRL/WS 07-0117, 05 Jan 2007.

14. ABSTRACT
A pulsed DC dielectric barrier discharge plasma actuator is investigated to reattach the simulated separated flow of a highly loaded turbine blade suction surface. Pulse rates of 25, 50, 75, and 100 pulses per second were investigated at a nominal constant pulse power of 8.5 kW for a constant pulse width of 250 ns. The separation of the flat plate boundary layer is induced with an adverse free stream pressure gradient distribution from an upper wall. Phase-locked particle image velocimetry (PIV) was used to obtain two-dimensional velocity field measurements at 6 to 24 equally spaced phase-angles, depending on the pulse rate. At a pulse rate of 100 pulses per second the 70 % velocity contour in the boundary layer was moved closer to the wall by 39%, compared to the unforced case, 15 mm downstream of the actuator.

15. SUBJECT TERMS

16. SECURITY CLASSIFICATION OF:			17. LIMITATION OF ABSTRACT:	18. NUMBER OF PAGES	19a. NAME OF RESPONSIBLE PERSON (Monitor)
a. REPORT	b. ABSTRACT	c. THIS PAGE			Rolf Sondergaard
Unclassified	Unclassified	Unclassified	SAR	16	19b. TELEPHONE NUMBER *(Include Area Code)* N/A

Standard Form 298 (Rev. 8-98)
Prescribed by ANSI Std. Z39-18

45th AIAA Aerospace Sciences Meeting and Exhibit
8-11 January 2007, Reno, Nevada

AIAA 2007-942

Effects of Pulsed-D.C. Discharge Plasma Actuators in a Separated Low Pressure Turbine Boundary Layer

J. D.Wall*
Air Force Institute of Technology Wright-Patterson AFB, Ohio, 45433

I. C. Boxx†, and R, B. Rivir‡
Air Force Research Laboratory, Wright-Patterson AFB, Ohio, 45433

and

M. E. Franke§
Air Force Institute of Technology Wright-Patterson AFB, Ohio, 45433

A pulsed DC dielectric barrier discharge plasma actuator is investigated to reattach the simulated separated flow of a highly loaded turbine blade suction surface. Pulse rates of 25, 50, 75, and 100 pulses per second were investigated at a nominal constant pulse power of 8.5 kW for a constant pulse width of 250 ns. The separation of the flat plate boundary layer is induced with an adverse free stream pressure gradient distribution from an upper wall. Phase-locked particle image velocimetry (PIV) was used to obtain two-dimensional velocity field measurements at 6 to 24 equally spaced phase-angles, depending on the pulse rate. At a pulse rate of 100 pulses per second the 70 % velocity contour in the boundary layer was moved closer to the wall by 39%, compared to the unforced case, 15 mm downstream of the actuator.

Nomenclature

c	=	blade chord length (m)
C_p	=	$(P_t - P_s)/(1/2\ \rho u^2)$
P_s	=	local static pressure (N/m^2)
P_t	=	total pressure (N/m^2)
Re_c	=	$\rho U_{inf} c/\mu$
Tu	=	$\sqrt{u'^2 + v'^2}\,/\sqrt{U^2 + V^2}$
U	=	local streamwise velocity (m/s)
U_{inf}	=	freestream velocity at infinity (m/s)
V	=	local freestream vertical velocity (m/s)
V_{inf}	=	freestream vertical velocity at infinity (m/s)
ρ	=	freestream air density (kg/m^3)
μ	=	viscosity (Ns/m^2)

I. Introduction

THE demands for greater performance and efficiency in low-pressure turbine blades has lead to higher airfoil loading. A limiting parameter for blade loading is the increased level of boundary layer separation at low Reynolds numbers. In an effort to maintain high blade loading, forestall flow-separation or reattach already separated flows over the Low Pressure Turbine (LPT) at low-Reynolds numbers, passive and active flow-control mechanisms have been investigated. Plasma excitation of the wall region offers a method of manipulating

*Ensign United States Navy, Air Force Institute of Technology / ENY, 2950 Hobson Way, WPAFB, OH 45433
†NRC Research Associate, AFRL/PRTT, 1950 Fifth Street, WPAFB OH 45433, AIAA Member.
‡ Senior Scientist, AFRL/PR, 1950 Fifth Street, WPAFB OH 45433, AIAA Associate Fellow.
§Professsor, Air Force Institute of Technology / ENY, 2950 Hobson Way WPAFB, OH 45433, AIAA Associate Fellow.

the near-wall velocity profile and to induce boundary layer reattachment. The effects of electrostatic fields on fluid flows have been demonstrated over many years. Velkolff[1] investigated electric field effects on heat transfer and pressure distributions for stagnation and flat plate boundary layer flows. Roth et al.[2] found that a dielectric barrier discharge (DBD) with an asymmetric electrode configuration mounted on a flat plate could reduce drag and also the overall boundary layer thickness by inducing local acceleration of fluid near the wall. Since then, a number of researchers have characterized the effect of these actuators on flow over aerodynamic surfaces. Corke et al.[3] studied flush mounted and subsurface plasma actuators as a means to introduce controlled disturbances into flow over axisymmetric bodies in supersonic flows of Mach numbers 3.5 and 6. Post et al.[4] studied plasma actuators as a means of controlling flow separation over a NACA $66_3 - 018$ airfoil over Reynolds numbers ranging from 77,000 to 460,000. They demonstrated an 8 degree increase in maximum angle of attack, accompanied by a full pressure recovery after stall. Post et al.[5] also studied the effect of plasma actuators on an oscillating NACA-0015 airfoil and were able to achieve a higher cycle-integrated lift.

Several investigations of the application of the DBD actuators to separated LPT cascade flows have been reported. Hultgren et al.[6] studied an array of asymmetric electrode DBD plasma actuators mounted on a flat plat in a simulated pressure field of the suction side of a Pak-B LPT blade at Reynolds numbers ranging from 50,000 to 300,000. They concluded their phased array DBD plasma actuator was an effective device for separation control on the LPT blade. List et al.[7] studied an asymmetric electrode DBD plasma actuator on a linear cascade of Langston turbine blades and found the actuators could reduce profile loss by 14% at low Reynolds numbers (Re = 30,000). Huang et al.[8] studied plasma actuators positioned at various chord locations on the surface of a Pak-B profile in a linear turbine cascade over Reynolds numbers ranging from Re_c = 10,000 to 100,000. They found the boundary layer flow reattachment point induced by the plasma actuator was highly sensitive to free stream turbulence and Reynolds number.

Although the studies above have produced useful insight into the effect of plasma actuators on a variety of boundary layer flows, they have relied almost entirely upon time-averaged measurements. While such measurements are useful in studying global effects and trends they also inevitably obscure the periodic nature of the physical mechanism through which these actuators force the near-wall boundary layer flow. Time-averaged measurements are particularly poor in determining what phase of the actuator cycle is dominant in affecting change in local and global flow field characteristics. For example, it has been noted by previous researchers (Rivir et al., [9] and Enloe et al., [10]) that clusters of very short duration, 10's of ns, current spikes form during the ignition phase of the DBD actuator cycle. Peak current during these events can be several orders of magnitude higher than the peak-to-peak current variation elsewhere in the cycle. Figure 1 shows a characteristic voltage and current trace measured in continuous AC DBD discharges.

The objective of the current study was to investigate pulsed dc discharges with low duty cycles to determine the sensitivity to duty cycle and power. In this study the power per pulse was held constant and the duty cycle varied. Pulsed DC discharges have been previously investigated in Rivir et al.[9] in quiescent air, for pulse lengths from 22 ns to 2 ms as illustrated in figures 2 and 3. These pulsed discharges have higher voltages, currents, and powers, during the pulse, typically 2-15 kW but also as high as 70 kW. In this effort the pulse width was standardized at 250 ns. The duty cycle was varied by varying the pulse rate from 25, 50, 75, to 100 Hz. This results in an average power variation from 0.05 to 0.2 watts. In contrast the continuous AC power levels varied from 5-25 watts. The plasma actuator was located in a well-characterized flow-field. The flow-field was a fully separated flat-plate boundary layer in a free stream pressure distribution designed to simulate that of a generic low-pressure turbine blade. The measurements used in this study included high spatial-resolution, phase-locked PIV and 31 pressure taps along the test section. Two-dimensional velocity field measurements were acquired at each of 6 to 24 points between plasma pulses. 2000 pairs of images were compared for each pulse rate points with the camera double frame framing rate at 600 frames per second. Low order frequency spectrums were compared for each pulse rate. The actuator reduced the boundary layer for all pulse rates investigated.

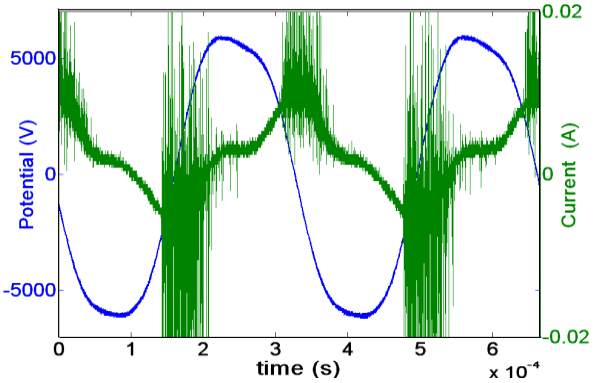

Figure 1. DBD cycle voltage and current .

II. Experimental Apparatus

A. Plasma Actuator

This experiment used the same facility and experimental apparatus which is described in detail in Boxx et al.[11,12]. The DBD flow-control actuator used in this study is shown in Figure 2.. It consisted of two copper electrodes separated by a layer of fiberglass laminate. The section of the electrodes where plasma is generated measured 95 mm by 3.2 mm wide and 0.036 mm thick. The fiberglass laminate separating them was 1.56 mm thick and had a dielectric strength of 28 kV/mm. The upper and lower electrodes do not overlap in the y-axis but are placed in an asymmetric configuration with the upper electrode on the upstream side and the lower one on the downstream. The line corresponding to the interface between the trailing edge of the upper electrode and the leading edge of the embedded is taken as the origin of the x-y coordinate system.

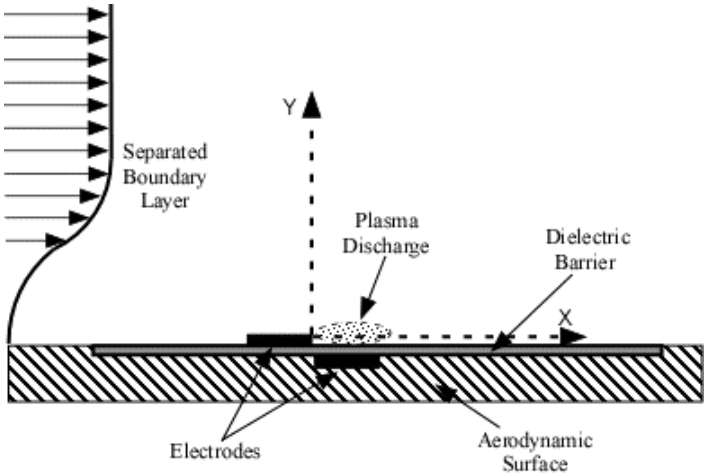

Figure 2. Schematic diagram of the dielectric barrier discharge flow-control actuator configuration.

The actuator was fabricated from a double-sided copper-clad circuit board using a photolithography technique. Actuators fabricated from this material are inexpensive to produce and allow highly accurate placement and alignment of the electrodes for a uniform discharge. The fiberglass laminate tends to degrade with increased exposure to the plasma discharge. The exposed electrode and circuit board surface were coated with a layer of high-temperature enamel. This protected the surface and resulted in a slight increase in the dielectric strength of the barrier. The electrodes were driven with a pulse-dc power circuit. This circuit is shown in Fig. 3. This circuit consisted of a 12kV, 0.33A Glassman DC power supply, a 25nF capacitor, and a Belhke model HTS-181 or a HTS 151 high-voltage solid state switch. The HTS-181 was used for all but the 100 pps measurements and is rated to 18kV and 60A. In the current study, voltage was fixed at 8.5kV. On-time for the switch was 250 ns. Electrical lead length and separation were minimized to reduce external circuit effects.

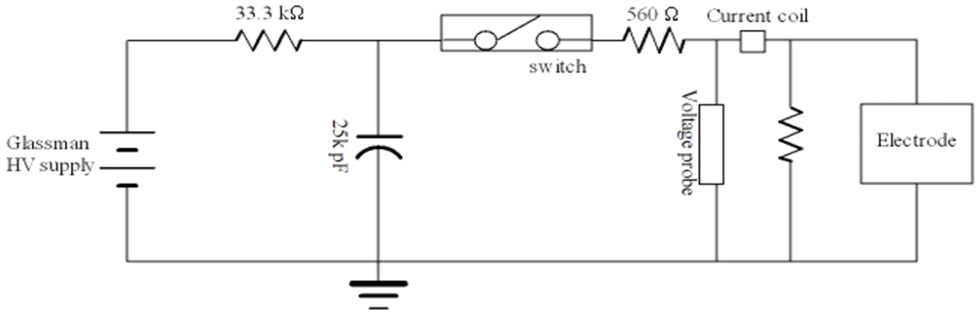

Figure 3. Pulsed-dc discharge power delivery circuit.

B. Low-Speed Wind Tunnel

All experiments were conducted in the low-speed wind-tunnel section of the Turbine Aero Thermal Basic Research Facility at the Air Force Research Laboratory. The low-speed wind-tunnel has a rectangular test-section measuring 38 ×25 cm. and its sides are 2.54 cm thick Plexiglas. The voltage was measured using a pair of 1000×

voltage-attenuation probes, Tektronics Model P6015A. Current was measured with a Pearson Model 4100 current coil. In order to correct for induction and capacitance inherent in the power-conditioning, a baseline case using a series of low-impedance pure resistors in place of the actuator was also utilized to make reference power loses in the circuit.

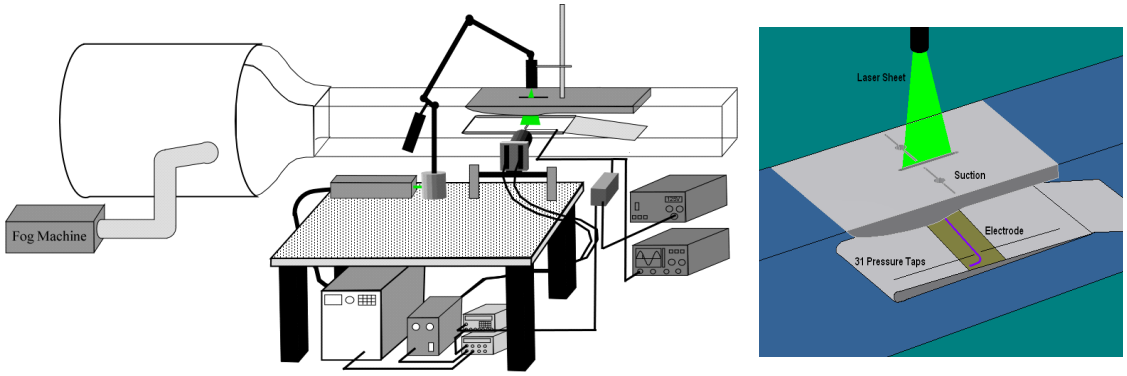

Figure 4. Experiment configuration, showing low-speed wind tunnel, PIV system and plasma actuator switch components.

Temperature of the flow through the tunnel was regulated and set to 26.6 ˚ C using a water-cooled chiller. Flow through the facility was seeded with propylene-glycol/water droplets (nominally 4 μm diameter) from a Rosco Model 4500 fog generator. The actuator was mounted on a flat plate located in the test-section of the tunnel. A recess milled into the upper surface of the plate ensured the actuator was flush with the surface. The active the plasma-generating region of the actuator spanned only the center 95 mm of the plate in order to avoid wall-effects from the sides of the tunnel.

The upper wall of the tunnel was contoured to provide the suction surface pressure distribution approximating that of a generic aft-loaded, low-pressure turbine blade. The upper tunnel wall was fabricated with a rapid prototype insert that provided a slot to provide suction to create the separation on the flat test surface and a slot for the laser light sheet. In order to keep flow attached over the contour a vacuum was applied to a 6.25 mm long slot which spans the width of the block downstream of the throat of the contoured section. The laser light sheet window was closed with a Plexiglas window contoured to the wall. The ssuction was generated using a throttled, 2HP vacuum system. The flat plate test section has a 4/1 elliptical leading edge and 31 offset pressure taps, located out of the side wall boundary layer. The electrode structure was located at the 63% axial chord location and downstream of the initial separation location.

C. PIV System

The PIV system used a dual-head, frequency-doubled, flash lamp-pumped Nd:YAG laser, New Wave Pegesus, and an adjustable light-arm to deliver sheet-illumination to the test-section. Light scattered from propylene-glycol seeding droplets was imaged with a high frame rate, 1024 × 1024 pixel resolution Photron-APX CMOS camera. The camera was triggered in a two-frame burst mode to produce a frame-straddling PIV system. The camera was equipped with a 200 mm lens, Nikon, AF-Nikkor, operating at f/11. The field of view of the PIV system was 17.9 × 17.9 mm. Each pixel corresponds to 17.45 μm in physical space for approximately 1-to-1 imaging. The camera and lasers were synchronized using two pulse/delay-generator timing boxes, Stanford Research Systems DG-535 and Quantum Composers 9300 Series respectively. The images were processed with Dantec's Flow Manager with a adaptive window offset cross-correlation algorithm. The final window size was 32 × 32 pixels with 50% overlap for a final spatial resolution of ≈ 0.56 mm and vector placement every ≈ 0.28 mm. The data was then post-processed using in-house codes.

D. Boundary Conditions

The driver signal for the DBD actuator in this study was set to a pulse length of 250 ns and had a peak-to-peak potential difference of 8.5kV. The local free stream velocity above the actuator location was nominally 1.8 m/s and Tu = 4.6% ($Tu = \sqrt{u'^2 + v'^2} / \sqrt{U^2 + V^2}$, where U and V are the local free stream velocity components in the x and y directions). The static-pressure distribution along the test-section wall was measured at 31 points using a

GE - Druck LPM 9481, 0.2" H_2O full-scale range pressure transducer in a Scanivalve. These pressures were used to compute the C_p distribution shown in the plot presented in Fig. 5. C_p was defined as $C_p = (P_t - P_s) / (\frac{1}{2}\rho U^2)$, where U is the free stream velocity upstream of the actuator. As noted above, suction was applied to the contoured upper surface of the wind-tunnel test-section in order to prevent flow-separation there. The plot shown in Fig. 5 also shows the C_p distribution for the case where no suction was applied to the upper surface. It can be seen from the similarity of the two profiles that although the applied suction resulted in an attached flow over the upper surface, it did not result in a substantial alteration of the free stream pressure characteristics. Comparing our measured C_p distribution to that of a generic low-pressure turbine airfoil, we determined that the contoured test-section produced and effective chord length of 35 cm, resulting in a simulated chord-Reynolds number of 23,500 for this study.

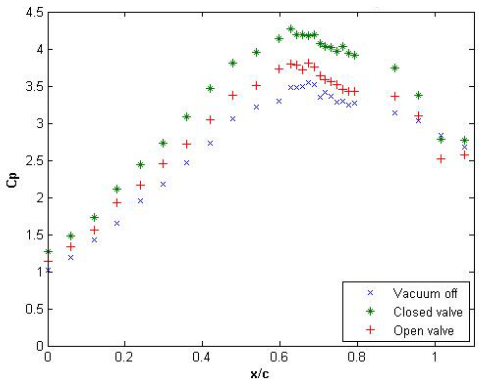

Figure 5. Cp distributions for simulated test section.

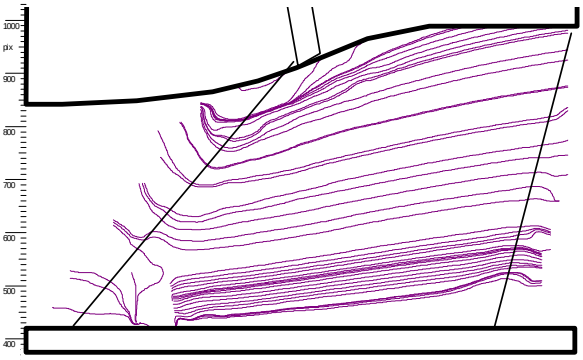

Figure 6. Streamlines of flow through the test-section in the vicinity of the actuator. The dashed lines show the approximate location laser-sheet cutoff, where particle-dropout was seen to result in a region of lower SNR.

In order to better characterize the nature of the flow through the test-section, we also performed a series of wide-field PIV measurements using the system described above. The streamlines derived from these measurements are shown in Fig. 6. Overlaid on these streamlines are the relative positions of the contoured upper section of the wind-tunnel, including the slot where the suction was applied, and the outer bounds of the laser sheet illumination. The signal-to-noise ratio of the measurements dropped off quickly at the edges of the laser sheet, which results in the misshapen streamlines. It is clear from these streamlines that the suction applied to the contoured upper section of the tunnel induced a small but noticeable, ≈ 0.2m/s velocity in the vertical direction. Although this added vertical velocity was undesirable it was necessary in order to maintain stability and uniformity in the test-section. The vertical velocity induced by suction provided an additional challenge to flow-reattachment.

III. Results and Discussion

A. Pulsed DC Voltage, Current, Power, Velocity Measurements

22 ns pulses and 2 µs pulses are shown in Fig. 7 and 8 for the HTS-151 switch at a duty cycle of 100 pps. Duty cycle and pps will be used interchangeably and is defined as the % time the plasma is on per second. This provides an average power of ~1watt at this pulse rate with a peak power of 60 kW/pulse and an average of 2-7 kW/pulse. The HTS-151 switch was used to provide the 100 pps measurements. The streamlines with plasma on and off are shown in Fig. 9 and the contours of the 70% boundary layer streamline are shown in figure 10 for a 250 ns pulsed at 100 pps at an average power of 0.213 watts compared against the continuous AC discharge at a power of ~5 -25 watts. The HTS-181 was more difficult to characterize due to changes in the external circuit which resulted in oscillations.

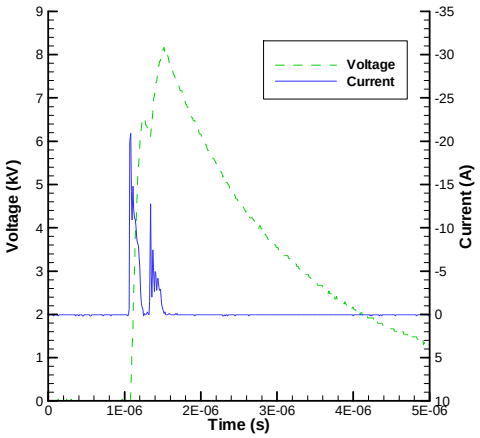

Figure 7. 22 ns pulse HTS-151.

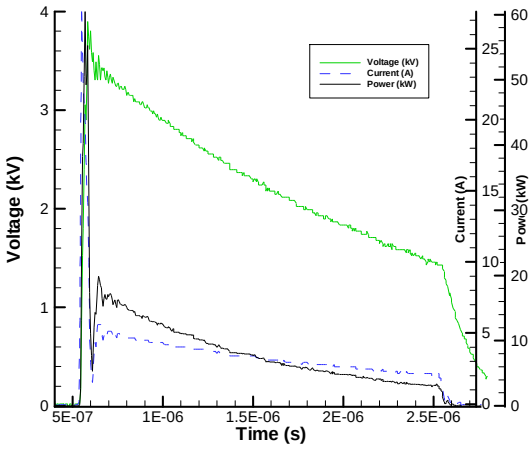

Figure 8. 2 µ second pulse HTS-151.

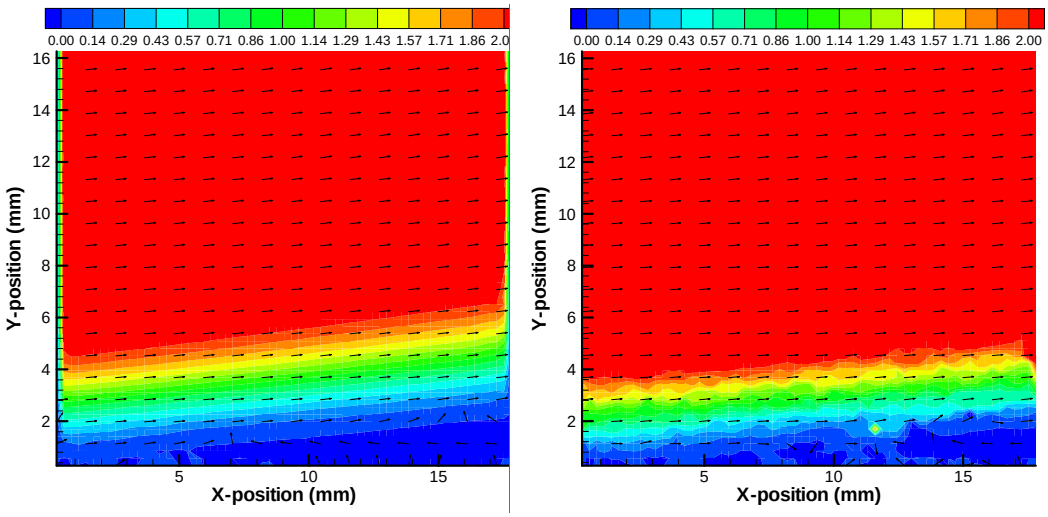

Figure 9. Comparison of streamlines plasma off and on HTS-151 250 ns pulse length @100 pps.

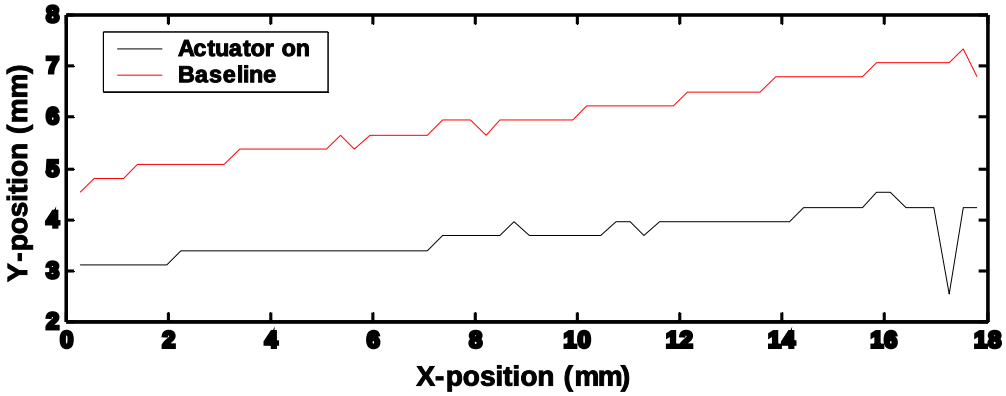

Figure 10. 70% contour HTS-151 with a 250 ns pulse length @100 pps.

While the separation was not entirely eliminated, for all duty cycles evaluated, 25, 50, 75, 100 pps (average power = 0.053, 0.011, 0.159, 0.213 watts, respectively), the 70 % contour was always reduced and moved closer to the wall. The lower duty cycles were evaluated with the HTS-181 switch in place of the HTS-151. The HTS-151 failed following 100 pps testing. The HTS-181 has a voltage and current rating, 18 kV and 60 A. Long delivery

times precluded immediate replacement of the 151 switch. The same pulse length, 250 ns was used for the HTS-181 switch. The continuous AC case is shown in Fig. 11 for comparison at a power level of ~25 watts and the magnitude reduction of the 70 % contour is extrapolated from the 50% reduction at x=10 mm to 54% at x =15mm. The average power level in the pulsed case is 0.213 watts, two orders of magnitude less than the continuous case from Boxx et al.[11,12]. The duty cycles from 25 to 100 pps 70 % contours are summarized in Fig. 12 and 13. The 75 Hertz case at 70% is suspect as all other 75 Hertz cases show similar ~ 17-23% reductions.

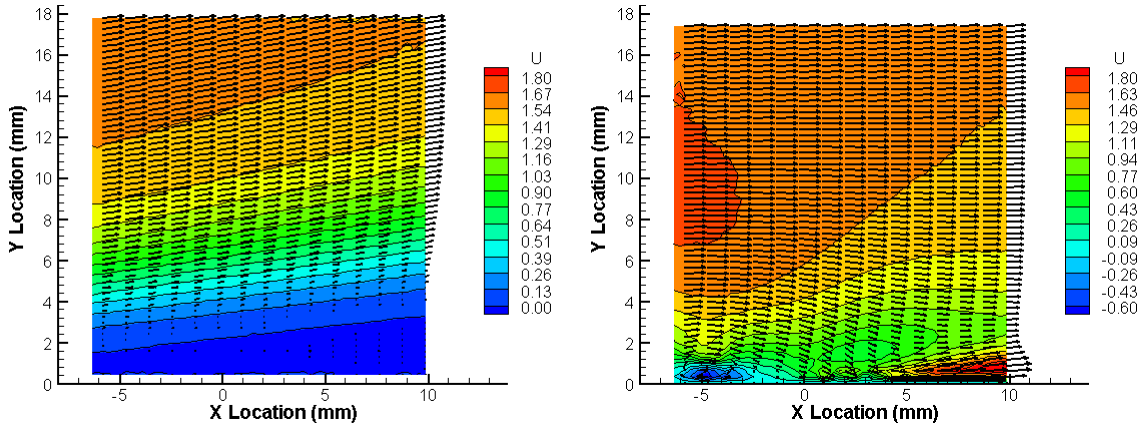

Figure 11. Separated flow actuator off / attached flow actuator on continuous 3 kHz, 25 Watts, U m/s 70% velocity contour attenuated 50%, x = 10mm, extrapolated to 54%, x = 15 mm.

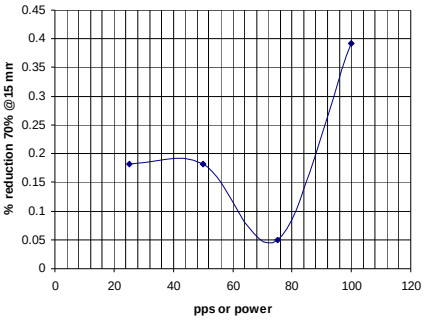

Figure 12. 70% contour reduction @ x = 15mm.

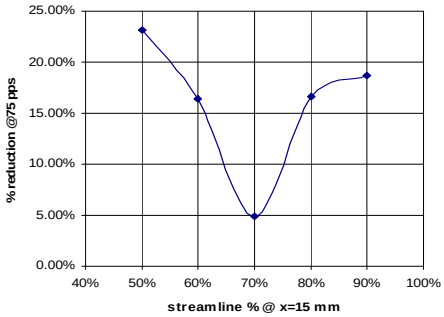

Figure 13. Streamline % @ x = 15mm @ 75 pps.

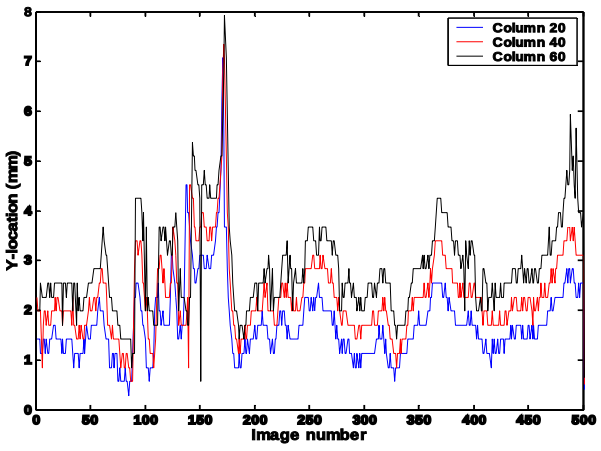

Figure 14. Plasma off contours with time.

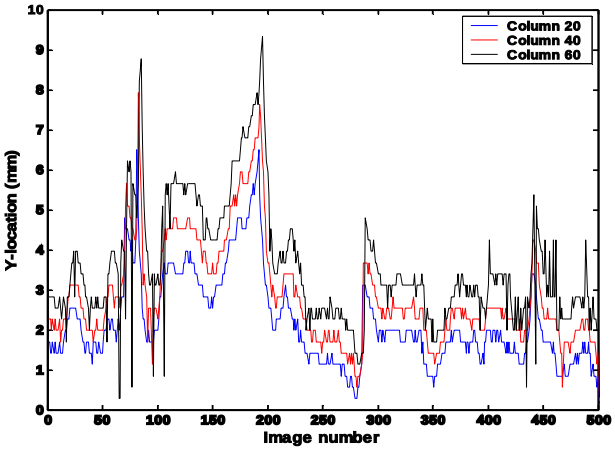

Figure 15. Plasma on contours with time.

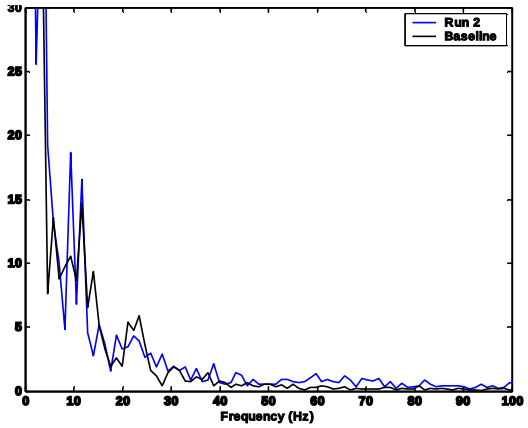

Figure 16. Frequency spectrum using 5 series @100pps

Phase locked measurements were possible with the continuous AC experiments using multiple pulses. The double frame time for PIV was 100 µ seconds to allow accurate resolution of the nominal 2 m/s free stream velocities. The frame rate selected for the multiple frames was 600 Hz. 3000 Hz AC sources then have 3 double frames per cycle and the 0.250 µs pulse length DC pulses would have 6 to 24 double frames between pulses @100 and 25 pps. The pulse would be convected 0.6 mm (since the turbulent spot at the wall is convected at ~30% of free stream) to 2mm for the free stream downstream between camera frames or 3.6 to 12 mm between plasma pulses at 100 pps.

Figures 14 and 15 were created by taking columns (x or pixel number) at 20%, 40%, 60% of the PIV window and then plotting three curves for the 500 frames. Because the x coordinates are directly proportional to the pixel number and the camera framing rate is constant at 600 frames per second Fig. 14 and 15 can be converted to time and amplitude. The use of three columns results in a usable frequency spectrum of only 10 Hertz. In Fig. 16 five columns have been used to compute the frequency spectrum which allows resolution of frequencies of up to 20 Hertz. Previous experiments have shown the 10-20 Hertz frequencies to be characteristic of the shedding of the separation bubble.

IV. Conclusions

The effects of pulse rates of 100, 75, 50, and 25 pps were investigated at a constant pulse power in a simulated Pak B pressure distribution for a Re of 23,500. The pulse voltage was fixed at 8.5 kV and the pulse length at 250 ns, which resulted in a nominal 8.5 kW/pulse, or average powers of 0.213, 0.159, 0.106, and 0.053 watts respectively. The simulated pressure distribution resulted in separation upstream of 63% Cx where the actuator was located. Phase-locked particle image velocimetry (PIV) were used to obtain two-dimensional velocity field measurements at 6 to 24 equally spaced phase-angles, depending on the pulse rate. At a pulse rate of 100 pps the 70 % velocity contour in the boundary layer is moved closer to the wall by 39%, compared to the unforced case, 15 mm downstream of the actuator. Frequency spectrums with the plasma on showed expected separation bubble shedding frequencies and small increases in amplitude.

Acknowledgments

This work was performed under sponsorship from the Air Force Office of Scientific Research. The views and conclusions contained herein are those of the authors and should not be interpreted as necessarily representing the official policies or endorsements, expressed or implied, of the Air Force Office of Scientific Research or the U.S. Government. The DC pulsed DEB discharge measurements were accomplished as a part of Ensign Wall's AFIT Masters Thesis[13], and the PIV measurements on DEB DC and AC plasma discharges were thru the efforts of Dr. Isaac Boxx [11,12] during an NRC appointment to AFRL.

References

[1] Velkoff, H. R., "Investigation of the Effects of Electrostatic Fields on Heat Transfer and Boundary Lasers", Ph.D. Dissertation. Ohio State University, 1962.

[2] Roth, J.R., Sherman, D.M, Wilkinson, S.P. "Boundary Layer Flow Control With a One Atmosphere Uniform Flow Discharge Surface Plasma," AIAA 98-0328. 1998.

[3] Corke, T.C., Cavalieri, D.A. "Controlled Experiments on Instabilities and Transition to Turbulence in Supersonic Boundary Layers". AIAA 97-1817, 1997.

[4] Post, M. L., Corke, T.C. "Separation Control on High Angle of Attack Airfoil Using Plasma Actuators". 41st Aerospace Sciences Meeting and Exhibit, Reno NV. AIAA 2003-1024. 2003.

[5] Post, M.L., Corke, T.C., "Separation Control Using Plasma Actuators – Stationary and Oscillating Airfoils". AIAA 2004-0841. 2004.

[6] Hultgren, L.S., Ashpis, D.E. "Demonstration of Separation Delay with Glow-Discharge Plasma Actuators". 41st Aerospace Sciences Meeting and Exhibit, Reno NV. AIAA-2003-1025. 2003.

[7] List, J., Byerley, A.R., McLaughlin, T.E., van Dyken, R.D. "Using a Plasma Actuator to Control Laminar Separation on a Linear Cascade Turbine Blade". 41 Aerospace Sciences Meeting and Exhibit. Reno, NV. 2003.

[8] Huang, J., Corke, T.C., Thomas, F.O. "Plasma Actuators for Separation Control of Low Pressure Turbine Blades" AIAA 2003-1024, 2004.

[9] Rivir, R., White, A., Carter,C., Ganguly, B., Jacob, J., Forelines, A., Crafton, J., "AC and Pulsed Plasma Flow Control, " 41 Aerospace Sciences Meeting and Exhibit. Reno, NV, AIAA 2003-6055, 2003.

[10] Enloe, C.L., McLaughlin, T.E., VanDyken, R.D., Kachner, D., Jumper, E.J., Corke, T.C. "Mechanisms and Responses of a Single Dielectric Barrier Plasma Actuator: Plasma Morphology", AIAA Journal, Vol. 43(3). 2004.

[11] Boxx, I., Rivir, R., Newcamp, Lt J., Franke, M., Woods, N., "A PIV Study of a Plasma Discharge Flow Control Actuator on a Flat Plate in an Aggressive Pressure Induced Separation," GT 2006-91044, IGTI Barcelona, 2006.

[12] Boxx, I., Rivir, R., Newcamp, Lt J., Woods, N., "Reattachment of a Separated Boundary Layer on a Flat Plate in a Highly Ad\verse Pressure Gradient Using a Plasma Actuator," 3rd AIAA Flow Control Conference, June 2006.

[13] Wall, Ensign J. D., "An Experimental Study of a Pulsed DC Plasma Flow Control Actuator," AFIT GAE/ENY-06-J16 MS Thesis, June 2006.